

Dalton Transactions

Accepted Manuscript



This is an *Accepted Manuscript*, which has been through the Royal Society of Chemistry peer review process and has been accepted for publication.

Accepted Manuscripts are published online shortly after acceptance, before technical editing, formatting and proof reading. Using this free service, authors can make their results available to the community, in citable form, before we publish the edited article. We will replace this *Accepted Manuscript* with the edited and formatted *Advance Article* as soon as it is available.

You can find more information about *Accepted Manuscripts* in the [Information for Authors](#).

Please note that technical editing may introduce minor changes to the text and/or graphics, which may alter content. The journal's standard [Terms & Conditions](#) and the [Ethical guidelines](#) still apply. In no event shall the Royal Society of Chemistry be held responsible for any errors or omissions in this *Accepted Manuscript* or any consequences arising from the use of any information it contains.

COMMUNICATION

[Ru^V(NCN-Me)(bpy)(=O)]³⁺ Mediates Efficient C–H bond Oxidation from NADH Analogs in Aqueous Media rather than Water Oxidation

Cite this: DOI: 10.1039/x0xx00000x

Received 00th January 2012,
Accepted 00th January 2012Jully Patel,^a Karunamay Majee,^a Ejaz Ahamed,^a Koji Tanaka,^{*, b} and Sumanta Kumar Padhi^{*, a}

DOI: 10.1039/x0xx00000x

www.rsc.org/

The [Ru^V=O]³⁺ and [Ru^{VI}=O]⁴⁺ generated from [Ru^{II}(NCN-Me)(bpy)(H₂O)](PF₆)₂ (NCN-Me is the neutral N-methyl-3,5-di(2-pyridyl)pyridinium iodide after deprotonation of the C–H bond), plays the selective role in C–H bond oxidation of 2-(pyridin-2-yl)-9,10-dihydroacridine (PADHH) and water oxidation respectively.

The ubiquitous redox coenzyme NAD⁺/NADH couple is unique and fundamental due to its proton coupled electron transfer (PCET) reactivity. In biology, the C–H bond oxidation in NADH, plays the key role in electron transfer as well as proton transfer process.¹ Catalytic oxidation reactions by the ruthenium(IV)-oxo [Ru^{IV}=O]²⁺ intermediate complexes, have been extensively studied because of their wide range of stability at various pH. The hydride (H⁻), hydrogen atom (H[•]) and electron (e⁻) transfer have been implicated in various reactions of [Ru^{IV}=O]²⁺ by Meyer *et al* in acetonitrile media.^{2–4} The same effect has not yet been reported in aqueous media, which is the most favored medium by nature.

We report here that the six-coordinate Ru^{II}-aqua complex, [Ru^{II}(NCN-Me)(bpy)(H₂O)](PF₆)₂ (**1**, NCN-Me is the neutral N-methyl-3,5-di(2-pyridyl)pyridinium iodide after deprotonation of the C–H bond, Fig. 1), is a poor precursor-catalyst for water oxidation in presence of the oxidant ceric ammonium nitrate (CAN) at pH≈1.0. Highly oxidizing conditions are required to oxidize H₂O, but at the same time the water oxidation catalysts (WOCs) are decomposed and/or deactivated after a certain time span. The same issue was encountered with WOC **1**. But on the contrary complex **1**, acts as an efficient hydride releasing precursor-catalyst due to the easy access to high-valent ruthenium species.

The ligand NCN-Me was synthesized by a Pd-catalyzed cross coupling reaction of 2-(tri-*n*-butylstannyl)pyridine with 3,5-dibromopyridine followed by methylation by treating with CH₃I.^{5a} [Ru^{II}(NCN-Me)(bpy)(I)](PF₆) (**2**) was synthesized by treating one

equivalent of NCN-Me with the precursor complex [Ru^{II}(bpy)(DMSO)₂Cl₂] in ethanolic medium at 80 °C. The precursor complex [Ru^{II}(bpy)(DMSO)₂Cl₂] was prepared as per the reported procedure.^{5b} The NCN-Me coordinates as a neutral ligand after deprotonation from the central C–H bond (Fig. S27). The deiodination of [Ru^{II}(NCN-Me)(bpy)(I)](PF₆) (**2**) by AgPF₆ in water/acetone mixture (1:4, v/v) generates the aqua complex [Ru^{II}(NCN-Me)(bpy)(OH₂)](PF₆)₂ (**1**)

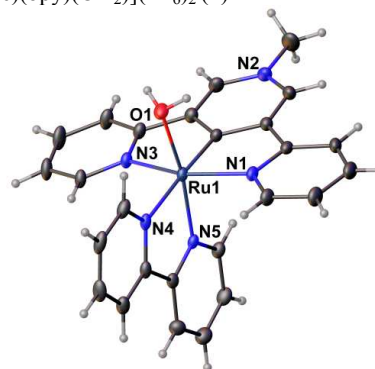


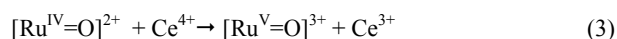
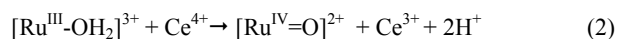
Fig. 1. ORTEP (30 %) of [Ru^{II}(NCN-Me)(bpy)(OH₂)]²⁺.

The complex **1** exists as Ru^{III}-OH₂ at pH≈1.0 phosphate buffer, where the resting potential appeared at 0.478 V vs. SCE. The rapid oxidation of the complex from [Ru^{II}-OH₂]²⁺ to [Ru^{III}-OH₂]³⁺ might have caused by aerial oxygen.⁶ The redox couples for Ru^{II}/Ru^{III}, Ru^{III}/Ru^{IV}, Ru^{IV}/Ru^V and Ru^V/Ru^{VI} were respectively observed at 0.37, 0.53, 0.69 and 1.02 V vs. SCE (Fig. 2). The pH dependent electrochemical properties of **1** reveals that upto pH ≈ 2.9, only one electron transfer occurs from Ru^{II}-OH₂/ Ru^{III}-OH₂ and the potential remains constant at 0.34 V vs. SCE. A slope of 60 mV/pH observed

for the $1e^-/1H^+$ coupled redox process between $Ru^{II}-OH_2/Ru^{III}-OH$ from pH 2.9-10.5. The pK_a of $Ru^{II}-OH_2 \rightleftharpoons Ru^{II}-OH$ and $Ru^{III}-OH_2 \rightleftharpoons Ru^{III}-OH$ were respectively observed at 10.5 and 2.9 from the pourbaix diagram. The observed slope of 60 mV/pH between pH 2.9-10.5 separated by a potential of 117 mV parallel to $Ru^{II}-OH_2/Ru^{III}-OH$ line was assigned to $Ru^{III}-OH/Ru^{IV}=O$. The one electron transfer processes of $Ru^{IV}=O/Ru^{V}=O$ and $Ru^{V}=O/Ru^{VI}=O$ were respectively observed at 0.7 V and 1.01 V vs. SCE (Fig. S12). The regions at pH \approx 2.9 and 10.5 were cross verified by phthalate buffer and borate buffer several times using a constant ionic strength and the data were added to the respective potentials. The complexes were dissolved in a degassed solvent containing the necessary amount of the supporting electrolyte. Single buffer of H_3PO_4 was used with the sequential addition of KOH. The minimum ionic strength of 0.1 M was maintained with the addition of KPF_6 into the aqueous solution. The bulk electrolysis (Fig. S13) were carried out in support of electron transfer reactions at 1.10 V and 0.95 V vs. SCE and pH \approx 1.6. The calculated electrons were respectively 3-electron and 2-electron oxidation at potentials 1.10 V and 0.95 V vs. SCE.

Tanaka and coworkers have already established the NCN-Me containing ruthenium NHC complex.^{5a,7} In case of complex **1**, the Ru-C resonance in ^{13}C NMR observed at, $\delta = 236.8$ ppm. This is suggesting the Ru-pyridinylidene structure in complex **1**. This coordinating effect of NCN-Me as an NHC makes the sense of stabilizing the higher oxidation state ruthenium(VI)-oxo ($[Ru^{VI}=O]^{4+}$) or ruthenium(V)-oxyl species ($[Ru^V-oxyl]^{3+}$) as inferred from the pourbaix diagram.

The catalytic water oxidation was carried out in pH \approx 1.0 triflic acid considering the precursor-catalyst **1** (1mM) and corresponding 100 equivalent of CAN. The catalyst either decomposed and/or deactivated after a certain time span. This in fact suggests that the ruthenium (VI)-oxo ($[Ru^{VI}=O]^{4+}$) species or ruthenium(V)-oxyl species ($[Ru^V-oxyl]^{3+}$), is generated and involved in the catalytic cycle of H_2O oxidation which differs from a majority of the reported catalysts for H_2O oxidation, where ruthenium(V) state, is the catalytically important intermediate. The instability of $[Ru^{VI}=O]^{4+}$ makes the system weaker to catalyze water. At a 1:100 catalyst/oxidant ratio (1 mM precursor-catalyst), TON of 2.25 was observed out of 25. But upon dilution catalyst deactivation is efficiently suppressed. At a 1:833 catalysts/oxidant ratio (0.03 mM precursor-catalyst), the turnover numbers (TONs) increased substantially up to 68 out of 208 (Fig. S15). The catalysis was monitored on a differential pressure transducer and O_2 evolution was confirmed through gas chromatograph. The rate of the O_2 (in μ mol) evolution was studied both with respect to catalyst as well as CAN concentration. A first order kinetics was observed in both the cases, where $k_{obs} = 16.5 \times 10^{-4} s^{-1}$ and $0.18 \times 10^{-4} s^{-1}$ respectively for precursor-catalyst and CAN concentration (Fig. S16-19). Oxidation to $[Ru^{VI}=O]^{4+}$ triggers water oxidation with added Ce^{IV} . The resting potential in pH \approx 1.0 HNO_3 was 0.364 V vs. SCE. Addition of 1 equiv of Ce^{IV} to a solution of 0.05 mM $[Ru^{II}(NCN-Me)(bpy)(H_2O)](PF_6)_2$ in HNO_3 ($\lambda_{max} = 461$ nm, $\epsilon = 5960 M^{-1} cm^{-1}$) results in the formation of $[Ru^{III}(NCN-Me)(bpy)(H_2O)]^{3+}$ ($\lambda_{max} = 461$ nm, $\epsilon = 2240 M^{-1} cm^{-1}$) (eq 1). Further the iterative addition of each 1 equiv of Ce^{IV} generates $[Ru^{IV}=O]^{2+}$ ($\lambda_{max} = 325$ nm, $\epsilon = 680 M^{-1} cm^{-1}$), and $[Ru^V=O]^{3+}$ ($\lambda_{max} = 325$ nm, $\epsilon = 580 M^{-1} cm^{-1}$) (eqs 2-3) (Fig. S9-11). An increase in the spectral band at 325 and 310 nm were observed during the change from $[Ru^{IV}=O]^{2+}$ to $[Ru^V=O]^{3+}$. There was no significant spectral change observed after the addition of one equiv. of Ce^{IV} into $[Ru^V=O]^{3+}$. This may be due to the less stability of $[Ru^{VI}=O]^{4+}$ at this condition.



From the open circuit potential (OCP) test it was observed that with the stoichiometric addition of three equivalents of CAN with respect to the precursor-catalyst **1** (1 mM) in an aqueous triflic acid solution at pH \approx 1, the resting potential jumped from 0.48 V to 1.00 V vs. SCE, but immediately started decaying the potential to 0.9 V vs. SCE within a time span of 1 minute. To the same solution another one equivalent of CAN was added, where the potential instantly raised to 1.00 V vs. SCE and decayed to 0.9 V vs. SCE within 10 secs. It signifies that the catalytic water oxidation started due to the active species $[Ru^{VI}=O]^{4+}$ species, but the sooner it arrives to the $[Ru^V=O]^{3+}$ state the process becomes saturated (Fig. S22). In this case the stability of $[Ru^{VI}=O]^{4+}$ species couldn't be controlled at our effort to afford higher catalytic effect towards water oxidation.

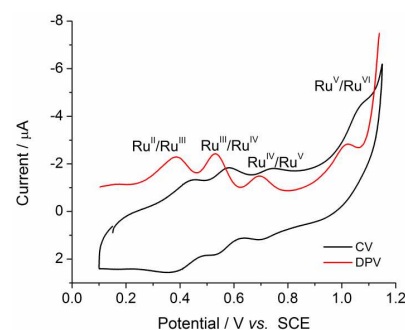
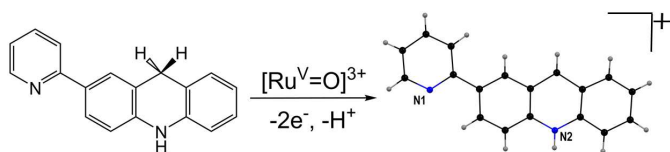


Fig. 2. CV and DPV of 0.5 mM $[Ru^{III}(NCN-Me)(bpy)(OH_2)]^{3+}$ at pH \approx 1.6.

The oxidation potential of PADHH under N_2 atmosphere is 0.75 V vs. SCE, (Fig. S24) and under acidic conditions it is 0.81 V vs. SCE, whereas the potential range for $[Ru^{IV}=O]^{2+}$ is below 0.7 V vs. SCE. This suggests that it is not possible for $[Ru^{IV}=O]^{2+}$ to oxidize PADHH. The redox couples for Ru^{IV}/Ru^V and Ru^V/Ru^{VI} were respectively observed at 0.69 and 1.02 V vs. SCE. It is pertinent to mention that $[Ru^V=O]^{3+}$ can be used to oxidize PADHH within the potential range 0.69-1.01 V vs. SCE. Therefore, the most stable intermediate $[Ru^V=O]^{3+}$ state was applied to release hydride from the NADH analog 2-(pyridin-2-yl)-9,10-dihydroacridine (PADHH). The behavior of PADHH is similar with NADH function, where PADHH can undergo a proton coupled two electron transfer to generate $PADH^+$. To a 1 mM solution of **1** in pH \approx 1 nitric acid, 3 equivalent of CAN added, and stirred for 5 minutes to generate $[Ru^V=O]^{3+}$ under aerobic conditions. A sample of prior dissolved 50 μ mol of PADHH in acetonitrile was added. It was allowed for stirring about 10 minutes. A saturated aqueous solution of KPF_6 was added to the mixture. A red colored crystals appeared after a week (Yield 35 %). The single crystal X-ray crystallography confirmed the formation of 2-(pyridin-2-yl)acridinium hexafluorophosphate, $[PADH]^+(PF_6)$ (Scheme 1).⁸ The UV-vis spectral changes monitored during the treatment of PADHH and *in situ* generated $[Ru^V=O]^{3+}$ in pH \approx 1.0 HNO_3 , with the addition of CAN to **1**. The reaction was much faster to control for kinetic analysis. Within 20 seconds the recorded two spectra for initial and final species indicates an increase in band at 460 nm (Fig. S22). The final spectra remain same after further scanning. The resulting spectra after the reaction between PADHH and $[Ru^V=O]^{3+}$ is almost similar to the addition spectra of individual spectra for $[Ru^{III}-OH_2]^{3+}$ and $[PADH]^+(PF_6)$ (Fig. S23). This suggests that, $[Ru^V=O]^{3+}$ state after accepting the hydride from PADHH, converts to $[Ru^{III}-OH_2]^{3+}$ along with $[PADH]^+$ (Scheme 1).

Scheme 1. Oxidation of PADHH to [PADH]⁺.

The presence of PADHH⁺, was detected by EPR analysis. An EPR tube containing a 0.5 mM solution of [Ru^V=O]³⁺ in pH≈1.0 HNO₃ was purged with nitrogen for 10 min. PADHH (1 mM) was then added to the solution, which was precooled near the melting point of acetonitrile. The reaction mixture was immediately cooled to 77 K in a liquid N₂ dewar for EPR measurements. The *g* value was calibrated using a Mn²⁺ marker. The *g*-value of the observed spectrum was 2.0029 (Fig. S30). The generated [Ru^{IV}=O]²⁺ is EPR silent at low temperature. This is also agrees with the reported value for similar analogues.⁹

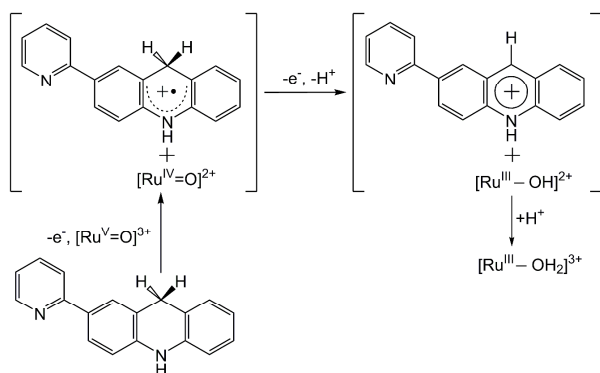
The effect of hydride release was analyzed in open circuit potential (OCP) test to study the resting potential. The aforementioned OCP test was continued to with the addition of 20 μmol solution of PADHH in acetonitrile. The resting potential of [Ru^V=O]³⁺ state at 0.9 V vs. SCE was sharply decreased to 0.50 V vs. SCE (Fig. S20). This actually suggests that the [Ru^V=O]³⁺ state after accepting the one proton coupled with two electrons from PADHH, converts to [Ru^{III}-OH]²⁺ state. Here the overall reaction is [Ru^V=O]³⁺ + 2e⁻ + H⁺ ⇌ [Ru^{III}-OH]²⁺, where [Ru^{III}-OH]²⁺ under acidic medium protonates to [Ru^{III}-OH₂]³⁺. In this case a proton coupled two electron transfer from PADHH to [Ru^V=O]³⁺ species occurs to generate [Ru^{III}-OH]²⁺ along with [PADH]⁺. It is expected that, the whole process occur in a stepwise manner;

Step 1: Reduction of [Ru^V=O]³⁺ to [Ru^{IV}=O]²⁺ through one electron generating PADHH⁺;

Step 2: Proton coupled one electron transfer (PCET) to reduce [Ru^{IV}=O]²⁺ to [Ru^{III}-OH]²⁺ with the generation of PADH⁺.

A proposed mechanism for the oxidation of PADHH to [PADH]⁺(PF₆) is depicted in Scheme 2.

Scheme 2. Proposed mechanism for oxidation of PADHH



It has been reported that the oxidation of AcrH₂ into 10-methylacridone (AcrO).^{4c} AcrH₂ in presence of *cis*-[Ru^{IV}(bpy)₂(py)(O)]²⁺ undergoes hydrogen atom transfer reaction followed by electron transfer to generate AcrH⁺. The subsequent

reaction of AcrH⁺ with [Ru^{II}(bpy)₂(py)(OH)]⁺ affords 10-methylacridone (AcrO). But in this case PADHH generates the most stable species [PADH]⁺(PF₆) rather undergoing further oxidation to corresponding acridone. To generalize the catalytic effects, it was observed that [Ru^{VI}=O]⁴⁺ is the active intermediate for water oxidation. Once the catalyst deactivates, the process becomes saturated with low turnover number. In case of C–H bond oxidation in PADHH, [Ru^V=O]³⁺ state is the active intermediate, which converts PADHH into [PADH]⁺(PF₆) through a proton coupled two electron transfer path. This indicates that selectively complex **1**, can be utilized for C–H bond oxidation and water oxidation depending upon the oxidation state of the ruthenium-oxo species.

This work was supported by the Department of Science and Technology (DST) under Grant DST(105)/2014-2015/392/AC, supporting S.K.P. ISM, Dhanbad is acknowledged for the partial supporting by the Grant (FRS (45)/2013-2014/AC). JP, KM and EA are grateful to ISM for institute fellowships. SKP acknowledges CRF ISM, CIF IIT Guwahati, and CDRI, Lucknow for analytical facilities.

Notes and references

^aDepartment of Applied Chemistry, Indian School of Mines, Dhanbad, India, 826004, E-mail: padhi.sk.ac@ismdhanbad.ac.in.

^bInstitute for Integrated Cell-Material Sciences, Kyoto University, Advanced Chemical Technology Center in Kyoto (ACT Kyoto) jibuchou 105, Fushimiku, Kyoto 612-8374, Japan, E-mail: koji.tanaka@icems.kyoto-u.ac.jp.

Electronic Supplementary Information (ESI) available: [details of any supplementary information available should be included here]. See DOI: 10.1039/c000000x/

- (a) J. J. Warren, T. A. Tronic, J. M. Mayer, *Chem. Rev.* 2010, **110**, 6961. (b) P. Fromme, Photosynthetic Protein Complexes: A Structural Approach; Wiley-VCH: Weinheim, Germany, 2008. (c) D. R. Weinberg, C. J. Gagliardi, J. F. Hull, C. F. Murphy, C. A. Kent, B. C. Westlake, A. Paul, D. H. Ess, D. G. McCafferty, T. J. Meyer, *Chem. Rev.* 2012, **112**, 4016.
- (a) M. T. Zhang, T. Irebo, O. Johansson, L. Hammarström, *J. Am. Chem. Soc.* 2011, **133**, 13224. (b) T. J. Meyer, M. H. V. Huynh, *Inorg. Chem.* 2003, **42**, 8140-8160. (c) C-M. Che. V. W. W. Yam, *Adv. Transition Met. Coord. Chem.* 1996, **1**, 209-237. J. R. Bryant, J. M. Mayer, *J. Am. Chem. Soc.* 2003, **125**, 10351-10361.
- (a) L. Ebersson, M. Nilsson, *Acta Chem. Scand.* 1990, **44**, 1062-1070. (b) T. M. Bockman, S. M. Hubig, J. K. Kochi, *J. Am. Chem. Soc.* 1998, **120**, 2826-2830.
- (a) B. A. Moyer, T. J. Meyer, *Inorg. Chem.* 1981, **20**, 436-444. (b) J. C. Dobson, J. H. Helms, P. Doppelt, B. P. Sullivan; W. E. Hatfield, T. J. Meyer, *Inorg. Chem.* 1989, **28**, 2200-2204. (c) T. Matsuo, J. M. Mayer *Inorg. Chem.* 2005, **44**, 2150-2158.
- (a) T. Koizumi, T. Tomon, K. Tanaka, *Bull. Chem. Soc. Jpn.* 2003, **76**, 1969-1975. (b) M. Toyama, K. Inoue, S. Iwamatsu, N. Nagao, *Bull. Chem. Soc. Jpn.* 2006, **79**, 1525-1534.
- L. Duan, F. Bozoglian, S. Mandal, B. Stewart, T. Privalov, A. Llobet, L. Sun, *Nat. Chem.*, 2012, **4**, 418-423.
- (a) S. H. Wiedemann, J. C. Lewis, J. A. Ellman, R. G. Bergman, *J. Am. Chem. Soc.* 2006, **128**, 2452. (b) J. C. Lewis, R. G. Bergman, J. A. Ellman, *J. Am. Chem. Soc.* 2007, **129**, 5332.
- (a) S. K. Padhi, R. Fukuda, M. Ehara, K. Tanaka, *Inorg. Chem.*, 2012, **51**(15), 8091-8102. (b) S. K. Padhi, R. Fukuda, M. Ehara, K. Tanaka, *Inorg. Chem.* 2012, **51**(9), 5386-5392. (c) S. K. Padhi, K. Tanaka, *Inorg. Chem.* 2011, **50**(21), 10718-10723. (d) S. K. Padhi, K. Kobayashi, S. Masuno, K. Tanaka, *Inorg. Chem.* 2011, **50**(12), 5321-5323.
- (a) S. Fukuzumi, Y. Tokuda, T. Kitano, T. Okamoto, J. Otera, *J. Am. Chem. Soc.* 1993, **115**, 8960-8968. (b) S. Fukuzumi, H. Katano, Y-M. Lee, W. Nam, *J. Am. Chem. Soc.* 2008, **130**, 15134-15142.

Graphical Abstract



The [Ru^V=O]³⁺ and [Ru^{VI}=O]⁴⁺ generated from [Ru^{II}(NCN-Me)(bpy)(H₂O)](PF₆)₂ (**1**, neutral N-methyl-3,5-di(2-pyridyl)pyridinium iodide after deprotonation of the C–H bond), which plays the selective role in C–H bond oxidation of 2-(pyridin-2-yl)-9,10-dihydroacridine (PADHH) and water splitting respectively are reported.